

# Electro-mechanical Coupling in MEMS: Modeling and Experimental Validation

V. Rochus, J.-C. Golinval

*Structural Dynamics Research Group  
Department of Aerospace and Mechanical Engineering  
University of Liege, Liege, Belgium  
Email: [V.Rochus@ulg.ac.be](mailto:V.Rochus@ulg.ac.be), [JC.Golinval@ulg.ac.be](mailto:JC.Golinval@ulg.ac.be)*

## Abstract

This paper presents the advantages of a strong coupled formulation to model the electro-mechanical coupling appearing in MEMS. The classical modeling approach is to use a staggered methodology iterating between two different programs to obtain the solution of the coupled problem. In this research a strong coupled formulation is proposed and a tangent stiffness matrix of the whole problem is computed. Using this matrix, nonlinear algorithms such as the Riks-Crisfield algorithm may be applied to solve the static nonlinear problem and accurately determine the static pull-in voltage. Moreover, the natural frequencies may be computed around each equilibrium positions. The dynamic behavior of the structure may also be studied and two new parameters are defined: the dynamic pull-in voltage and the dynamic pull-in time. This strong coupled methodology deriving from variational principle may also be used for topology optimization and extended finite elements.

The contribution presented here is based on the following two papers:

1. V. Rochus, D.J. Rixen, J.-C. Golinval, On the Advantages of Using a Strong Coupling Variational Formulation to Model Electro-Mechanical Problem, *Thermal, Mechanical and Multiphysics Simulation and Experiments in Micro-Electronics and Micro-systems EuroSime 2006, Como, Italia, 2006*
2. V. Rochus, D.J. Rixen, J.-C. Golinval, Correlation of Experimental and Numerical Results on Electrostatically Actuated Micro-Beams, *Ninth International Conference on Modeling and Simulation of Microsystems, Boston, USA, 2006*

## 1. Introduction

MEMS are very small devices in which electric as well as mechanical, thermal and fluid phenomena appear and interact. Because of their microscopic scale, strong coupling effects arise between the different physical fields, and some forces, which were negligible at macroscopic scale, have to be taken into account. In order to accurately design such micro-electro-mechanical systems, it is important to handle the strong coupling between the electric and the mechanical fields. In order to understand the physical phenomena of electro-mechanical coupling, the reference problem shown in figure 1 is considered. It consists in a capacitor made of two parallel plates between which a voltage is applied. The upper plate is supported by a spring and the lower plate is

grounded. This mass-spring model is representative of the mode of operation of electrostatically-actuated MEMS devices.

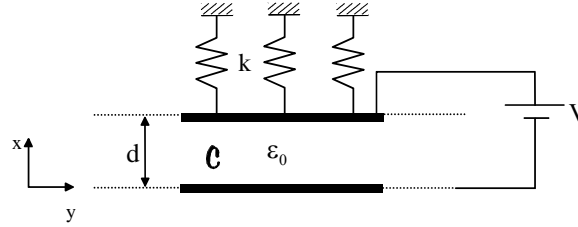


Figure 1: Reference Problem.

For the sake of simplicity, the electrodes of the capacitor are considered as infinite planes and the electric charges are supposed to be evenly distributed on the surfaces. This approximation allows the fringing fields to be neglected and the system is reduced to a one-dimensional problem. The capacitor is also considered to be in vacuum and no damping is considered in the model. The dynamic equilibrium equation of the system is [2]:

$$m\ddot{d} = -k(d - d_0) - \frac{1}{2} \epsilon_0 \frac{V^2}{d^2} \quad (1)$$

where  $d$  is the distance between the two plates;  $m$  is the mass of the upper electrode;  $k$  is the spring stiffness and  $\epsilon_0$  is the permittivity of free space. It can be noted from equation (1) that the dynamic behavior of the structure depends on the applied voltage  $V$  and on the initial gap between the plates  $d_0$ .

Let us consider the static equilibrium of the system. When the applied voltage increases, it creates an attraction force between the electrodes and the upper plate moves closer to the grounded plate. When the electric force in  $1/d^2$  becomes dominant with respect to the mechanical force so that the plates stick together, a critical voltage is reached. This critical voltage is called the static pull-in voltage. The analytical expressions of the static pull-in voltage and of the corresponding pull-in distance are given in [2]:

$$V_{pi} = \sqrt{\frac{8}{27} \frac{k d_0^3}{\epsilon_0}} \quad \text{and} \quad d_{pi} = \frac{2}{3} d_0$$

When the applied voltage  $V$  is smaller than the pull-in voltage, two equilibrium positions exist:  $d_e^{(1)}$  and  $d_e^{(2)}$  in figure 2. When  $V=V_{pi}$ , the two equilibrium positions merge into one point  $(d_{pi}, V_{pi})$ . Beyond  $V_{pi}$ , no equilibrium position exists.

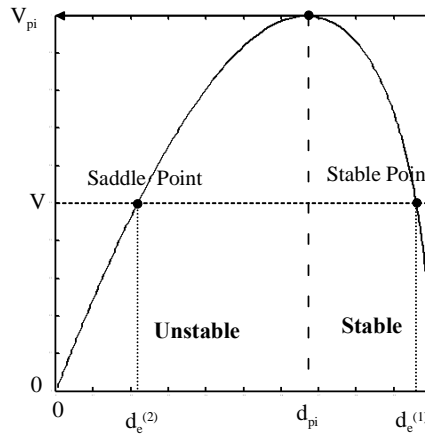


Figure 2: Pull-in Curve.

## 2. Numerical Methods

Classical methods used to simulate the coupling between electric and mechanical fields are usually based on staggered procedures, which consist in computing quasi-static configurations using two separate models as shown in figure 3 (a structural model loaded by electrostatic forces and an electrostatic model). Iterations are then performed: the electrostatic field is first computed using, for instance, the boundary element method or the finite element method and it provides the electrostatic forces acting on the mechanical structure. Then a mechanical FEM code computes the structure deformation under the effect of electric forces. The deformed structure defines new boundaries for the electrostatic problem and the electric field has to be computed again. This method is commonly presented in the literature (see e.g. Lee et al. [3]).

In this paper, a monolithically coupled electro-mechanical FE formulation is proposed, which allows the static equilibrium positions to be computed in a non-staggered way. The electric and mechanical fields are computed *simultaneously* in a unified formulation. Since the problem is non-linear, it must be solved by an iterative algorithm such as the Riks-Crisfield method. The solution strategy consists in the following steps. Given an electric potential applied on the boundaries of the structure, a first solution is obtained by considering the coupled problem linearized around an initial configuration. The resulting structural deformation then prescribes a modified electric domain and a new linearized problem is defined around the modified configuration. This process continues until the solution has converged, namely until the electric and mechanical equilibrium are satisfied up to a prescribed tolerance (Figure 4).

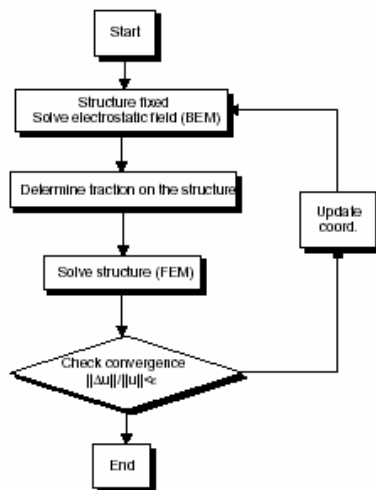


Figure 3: Staggered method procedure.

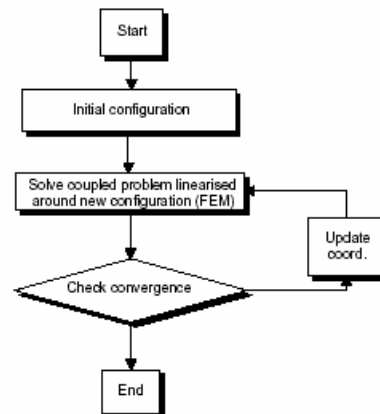


Figure 4: Monolithically method procedure.

### 2.1 Computation of Pull-in voltage

To approximate this critical voltage, the staggered method uses a “trial and error” methodology. To estimate the pull-in voltage, a voltage is first imposed and the algorithm searches the corresponding equilibrium position. If the algorithm converges to a solution, it means that the pull-in voltage is above the imposed voltage ( $V_i$  in figure 5). On the other hand, when the algorithm does not converge, one can conclude that the pull-in voltage is under the imposed voltage as in iteration  $i+1$  and so on until the pull-in voltage is approached. This method depends also on the robustness of the algorithm. Near the pull-in voltage, the problem becomes ill-conditioned since electric and mechanical stiffness contributions are nearly identical around the equilibrium point. The algorithm may therefore diverge before achieving the pull-in voltage. For this reason, the classical staggered method always underestimates the pull-in voltage.

In the strongly coupled method, the fact that the tangent stiffness matrix is available, allows to use path-following algorithms such as the Newton-Raphson method and the Riks-Crisfield technique [5]. Riks-Crisfield technique consists in constraining the distance between two computed points in the  $(d, V)$  graph to be at a predefined distance. Hence, instead of prescribing an increment in  $\Delta V_i$  from a previous equilibrium computation

corresponding to  $V_i$ , a new quasi-static equilibrium is searched for a combined increment in the driving parameter  $V_i + \Delta V_k$  and in the system unknown increments so that:

$$\mathbf{s}_k \cdot \mathbf{s}_k = \Delta S_i^2 \quad (2)$$

where  $\mathbf{s}_k$  locates the position of the point, with respect to point  $i$  and is defined by

$$\mathbf{s}_k = \begin{bmatrix} \Delta d_i + \Delta d_k \\ \Delta V_i - \Delta V_k \end{bmatrix} \quad (3)$$

This equation is a new constraint to add to the equilibrium equation. From this constraint, the incremental load  $\Delta V_i$  becomes an unknown of the problem and is modified during the process. When using such techniques it is possible to follow the voltage-displacement curve, pass over the pull-in voltage and enter in the unstable part of the curve (Figure 6). The pull-in voltage is thus well evaluated and the unstable curve gives the saddle points for different voltages.

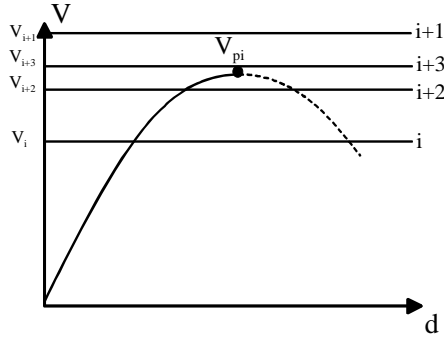


Figure 5: Pull-in evaluation with staggered method.

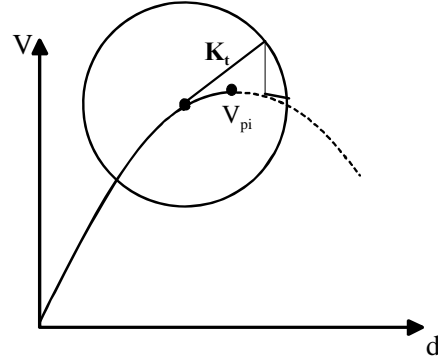


Figure 6: Pull-in evaluation with monolithically method.

## 2.2 Natural Frequency

The natural frequency of the coupled problem may be computed around each equilibrium position of the pull-in curve. Staggered methods compute the natural frequency by projecting the total equation on the first purely mechanical eigenmode. In the finite element formulation of the mechanical problem, the equation of the motion is:

$$\mathbf{M}\ddot{\mathbf{U}} + \mathbf{K}\mathbf{U} = \mathbf{F}_e(\Phi(\mathbf{U})) \quad (4)$$

where  $\mathbf{M}$  is the mass matrix and  $\mathbf{K}$  the stiffness matrix. The electric force  $\mathbf{F}_e$  depends on the electric potential  $\Phi$ . Since the boundary of the electric domain depends on the structural displacement,  $\Phi$  indirectly depends on  $\mathbf{U}$  and thereby generates an electric stiffness effect.

Let us consider the first mode  $\mathbf{Q}$  of the purely mechanical equation without electric force, namely the eigenvector satisfying  $(\mathbf{K} - \omega^2 \mathbf{M})\mathbf{Q} = 0$  for the lowest  $\omega$ . The structural displacements are then approximately represented by  $\mathbf{U} = \mathbf{Q}q$  where  $q$ , the amplitude of the displacement mode, is the generalized coordinate. The motion equation is thus reduced to a single-degree of freedom equation:

$$m\ddot{q} + kq = f_e \quad (5)$$

where  $k$ ,  $m$  and  $f_e$  are the reduced stiffness, mass and force corresponding to the assumed mode i.e.  $m = \mathbf{Q}^T \mathbf{M} \mathbf{Q}$ ,  $k = \mathbf{Q}^T \mathbf{K} \mathbf{Q}$  and  $f_e = \mathbf{Q}^T \mathbf{F}_e$ .

In order to find the linearized equation of motion and to derive the vibration frequency, one can evaluate the tangent stiffness  $k_e$  originating from the electric forces by finite difference. Applying a perturbation to the structural displacements of the form:  $\mathbf{U} = \mathbf{U}_0 + \mathbf{Q}\Delta q$ , ( $\mathbf{U}_0$  defining the static equilibrium configuration), one can compute the corresponding electric forces. The tangent stiffness  $k_e$  is obtained as follows:

$$k_e \cong -\frac{\Delta f_e}{\Delta q} = -\frac{\mathbf{Q}^T (\mathbf{F}_e(\Phi(\mathbf{U})) - \mathbf{F}_e(\Phi(\mathbf{U}_0)))}{\Delta q} \quad (6)$$

Finally the linearized equation for the assumed mode approach is  $m\Delta\ddot{q} + k\Delta q = \Delta f$  so that the approximate first eigenvalue is given by

$$\lambda \cong \frac{k - \frac{\partial f_e}{\partial q}}{m} \approx \frac{k + k_e}{m} \quad (7)$$

Obviously since the assumed displacement mode  $\mathbf{Q}$  corresponds to the purely structural mode, the eigenfrequency of the system is only approximated and one can show that it is always an upper bound of the frequency of the complete model. This method can be generalized easily to account for more than one assumed mode. This method is no more valid when the electrode is reduced to a small electrode under the beam. From the tangent stiffness matrix the frequencies may be easily computed for the strong coupled formulation.

### 3. Monolithically Finite Element Coupling

In this paper, we propose a finite element formulation to solve the electric and mechanical problems simultaneously in a strong-coupled form. One of the advantages of this formulation is that the tangent stiffness matrix of the electro-mechanical problem can be explicitly constructed. Thus, the natural frequency of the electro-mechanical system can be directly evaluated around a given equilibrium configuration and the transient dynamic response can be more easily computed.

The consistent way of deriving a finite element discretization to model electro-mechanical coupling consists in using the variational calculus. Starting from the energy of the coupled problem, nodal forces are obtained for an element by derivation of the energy. The tangent stiffness matrix of the coupled problem is then obtained by linearization of the equilibrium equations in the vicinity of an equilibrium position (see reference [2]):

$$\begin{pmatrix} \mathbf{K}_{uu}(\phi) & \mathbf{K}_{u\phi}(\phi) \\ \mathbf{K}_{\phi u}(\phi) & \mathbf{K}_{\phi\phi} \end{pmatrix} \begin{pmatrix} \Delta \mathbf{U} \\ \Delta \Phi \end{pmatrix} = \begin{pmatrix} \Delta \mathbf{F}_m \\ \Delta \mathbf{F}_e \end{pmatrix} \quad (8)$$

where subscripts  $u$  and  $\phi$  refer respectively to the mechanical and electric domains;  $\Delta \mathbf{U}$  is the displacement vector and  $\Delta \mathbf{F}_m$  is the vector of mechanical forces;  $\Delta \Phi$  is the electric potential vector and  $\Delta \mathbf{F}_e$  is the vector of electric forces. It can be observed that the tangent stiffness matrix is symmetric and that coupling terms such as  $\mathbf{K}_{u\phi}$  and  $\mathbf{K}_{\phi u}$  appear between mechanical and electric degrees of freedom. It should be noted that the tangent stiffness matrix, unlike in the common approach, is not obtained by finite difference, but derives naturally from the variational approach and can be easily assembled using the finite element model. More details about the expression of the coupling matrix may be found in reference [2].

### 4. Application to a Clamped-Clamped Beam

Let us consider the micro-bridge problem when a large distance of  $6 \mu\text{m}$  exists between electrodes and the thickness of the beam is about  $0.5 \mu\text{m}$  as shown in figure 3. Le length of the beam is about  $300 \mu\text{m}$ . Due to geometrical effects in the structural deformation, additional non-linearities are present. Large displacement hypothesis has to be considered. The static pull-in voltage, the natural frequency and the dynamic behavior of the system are significantly altered by geometrical stiffening. To model the mechanical structure, non-conforming elements and quadratic elements with large displacement hypothesis may be used.

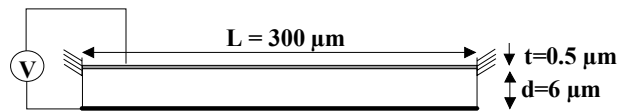


Figure 7: Clamped-clamped beam model.

#### 4.1 Static Equilibrium

A Riks-Crisfield algorithm is used to compute the variation of the displacement when the voltage varies and to estimate the value of the pull-in voltage. Because it comes from the static equilibrium equation, we will call this critical voltage, the *static pull-in voltage*. In the pull-in curve of figure 8, the dashed curve corresponds to the displacement of the middle point when deformation of the beam is assumed to be linear. In that case, the pull-in is estimated to around 18.4 V. The plain curve with dots represents the displacement when non-linear deformation effects due to the large displacements are accounted for. The static pull-in voltage is then estimated to 96.4 V. A difference of 80% is observed between the small displacement and the large displacement hypotheses. Hence it is essential to properly account for large displacements in this case.

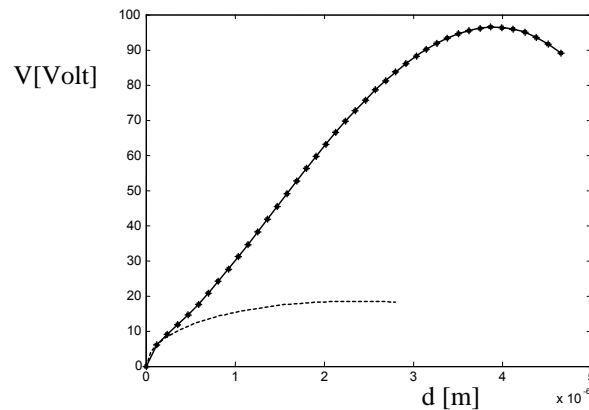


Figure 8: Pull-in curve for small displacements and large displacement hypotheses.

#### 4.2 Natural Frequency

The natural frequencies are also altered by the additional geometric stiffness. On the one hand, when the beam moves, the additional stiffness due to the geometric effect increases. The natural frequency then rises. On the other hand, when the beam approaches to the substrate, the electric forces increases and reduces the stiffness of the coupled problem. Figure 9 shows the evolution of the first five natural frequencies with the voltage. In small displacement hypothesis case the frequency decreases when the voltage increases. Here the frequency increases due to the additional geometric stiffness, but when the voltage increases so much that the electric force becomes dominant compared to the mechanical stiffness, the first natural frequency of the coupled problem decreases and becomes zero at the pull-in voltage.

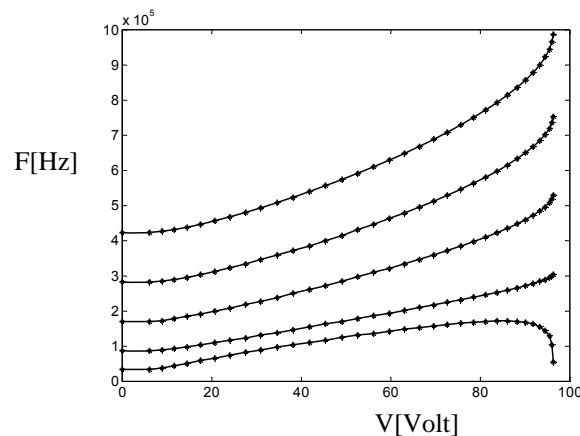


Figure 9: Evolution of the five first natural frequencies with the voltage.

*Comparison with the projection method*

To estimate the natural frequency, Lee et al. [3] use a projection method as presented in the previous section. Such a method is accurate when the electric force does not significantly influence the eigenmodes of the coupled structure. So, when the voltage is uniformly applied between the beam and the substrate, electric forces are uniformly distributed and the coupled electromechanical mode is almost similar to the purely mechanical mode. Computing the eigenfrequency of the system for different voltage levels, both methods yield very similar results. To observe a difference between the two methodologies, a different configuration of the electrodes is considered. The voltage is applied at the centered  $60\mu\text{m}$  length electrode as shown in figure 10.

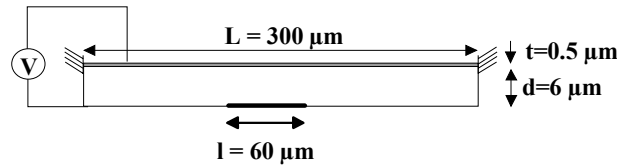


Figure 10: Reduced electrode model.

In figure 11 the first natural frequency evaluated by the power method is represented by dots and the projection method by circles. The difference between the two methods appears when the system comes closer to the pull-in.

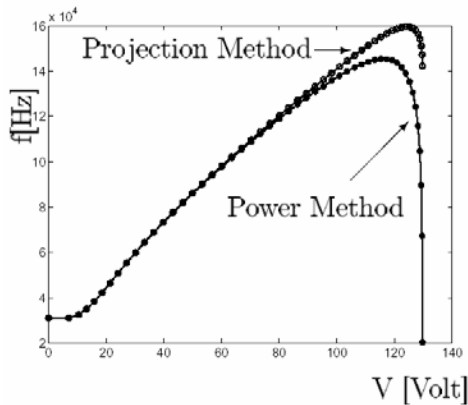


Figure 11: First natural frequency.

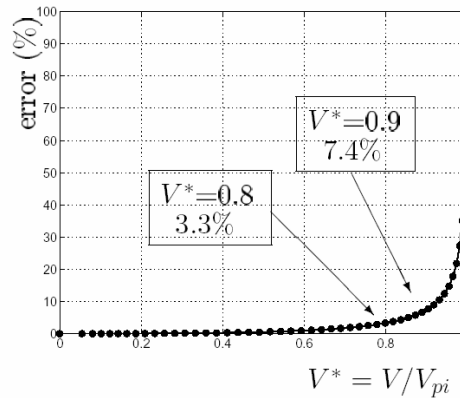


Figure 12: Relative error.

The relative error of the projection method in comparison with the strong coupled method is plotted in figure 12. When the system is at 80% of the pull-in voltage an error of 3.3% is observed. At 90% the error reaches 7.4%. This phenomenon may be explained by the different shape of the eigenmodes used in the two cases. Figure 14 shows the purely mechanical eigenvector (in gray) and the coupled mode (in black) at  $V^*=0.9$ . Large displacement increases the stiffness at the beam centre. Purely mechanical eigenmode shows an additional stiffness at this place. For the total coupled problem, the electric forces reduced the stiffness in the neighborhood of the electrodes. The two contributions compensate each other and the eigenmode is modified.



Figure 13: Electric potential for the reduced electrode at the static pull-in voltage.

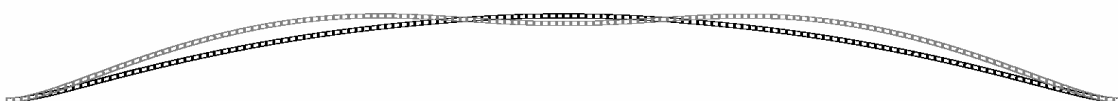


Figure 14: Eigenmodes with (black) and without (gray) electric force when  $V^*=0.9$  is applied to the centered electrode.

### 4.3 Dynamic Behavior

In this section, the transient dynamic response of the system is computed when the voltage is suddenly applied between the two electrodes i.e. when the time-history of the voltage corresponds to a step function as illustrated in figure 15. To investigate the dynamic pull-in, several voltages  $V$  were considered and applied to the beam as a step in time, the system being at rest initially. Using Newmark's scheme [4] to time-integrate the problem, one obtains the results depicted in the phase plot of figure 16.

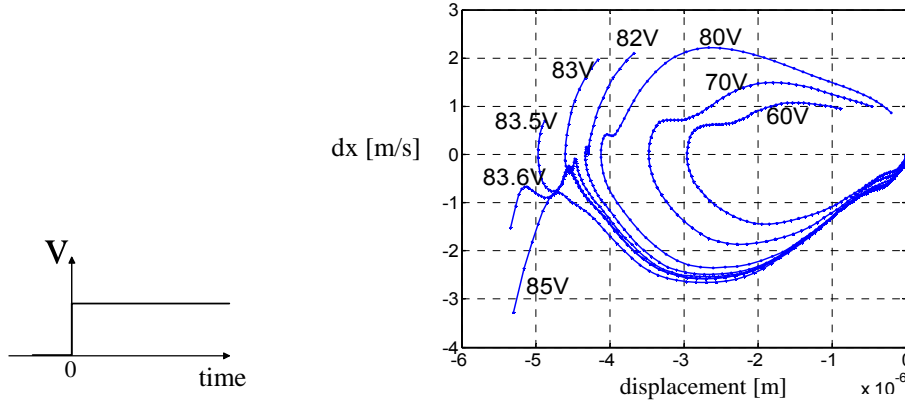


Figure 15: Step of voltage applied to the beam

Figure 16: Phase diagram for transient displacement of the middle node when a step of voltage is applied.

From the dynamic study of the electrostatically actuated beam behavior, two new parameters are defined the dynamic pull-in voltage and the dynamic pull-in time. The definitions are the following:

*The dynamic pull-in voltage is defined as the voltage amplitude such that, when applied suddenly, it leads to the dynamical instability of the system.*

*The pull-in time is defined as the time needed for the plates to stick together when the pull-in voltage is applied.*

In figure 16 the dynamic instability appears for a voltage of 83.6 V. This is the dynamic pull-in voltage. Its value is 13 % lower than the static pull-in voltage. The pull-in time is estimated to be  $1.4 \cdot 10^{-5}$  s.

## 5 Experimental Validation

The numerical simulations are now validated through the comparison with experimental results. MEMS were fabricated using the PolyMUMPS (Polysilicon Multi-User MEMS Processes) technology. The design and testing of these devices were performed at IEF ("Institut d'Electronique Fondamentale"), which is a CNRS research centre located in Paris. Different designs and structures were fabricated, but only the electrostatic actuated beams namely one electrostatic micro-bridge made in the first Polysilicon layer called Poly1, and two cantilever beams, one made in the first Polysilicon layer (Poly1) and one in the second one (Poly2) are considered here. The material characteristics and the dimensions of the micro-beams are given in table 1.  $L$  is the length of the beam,  $t$  the thickness and  $d$  the gap.  $L_{elec}$  is the length of the lower electrode deposited on the substrate. A picture of the studied micro-bridges is shown in Figure 17.



Polysilicon Properties			
E	158± 10 GPa	$\nu$	0.22±0.01
Poly 1 Micro-Bridge			
L	200µm	t	2.19 µm
L <sub>elec</sub>	100µm	d	1.87 µm
Poly 1 Cantilever Micro-Beam			
L	175µm	t	2.5 µm
L <sub>elec</sub>	168µm	d	1.87 µm
Poly 2 Cantilever Micro-Beam			
L	175µm	t	1.4µm
L <sub>elec</sub>	168µm	d	2.6µm

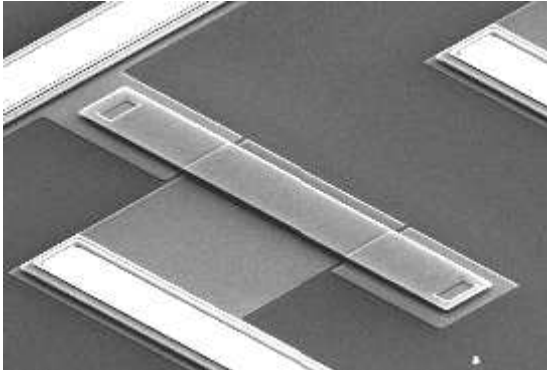


Figure 17: Dimensions and characteristics of the studied micro-devices.

### 5.1 Micro-Bridge

The first type of structure considered here is a micro-bridge. Pre-stress is present in the layer due to the fabrication process. A buckling effect may be observed, and a displacement of about 164 µm is measured at the beam centre.

#### *Buckling Simulation*

The first step to model these micro-devices is to estimate the pre-stress induced in the mechanical structure by the fabrication process. To determine exactly the stress distribution on the thickness of the beam the entire process should be simulated. In this study, only a mean pre-stress will be added to the structure. The solution of the problem is found using the Riks-Crisfield algorithm. A 30 MPa pre-stress is necessary to achieve the 164 nm initial displacement at the centre of the beam. The deformation of the beam due to the pre-stress is shown in Figure 18.



Figure 18: Initial deformation of the structure due to the pre-stress (10x).

#### *Pull-in Curve*

Starting from the buckled configuration a voltage is applied between the electrode and the beam. The electro-mechanical problem is solved using a Riks-Crisfield algorithm. The exact geometry of the anchor was not accurately measured. The different geometries presented in Figure 19 were considered. For each one the mean pre-stress is adapted to obtain the observed initial deformation. The displacements of the beam centre when the voltage increases are plotted in Figure 19 for each anchor shape. The geometry of the anchor has thus a certain effect on the pull-in curve. In Figure 19 the numerical results represented by dots, diamonds and squares overestimate the experimental data represented by circles.

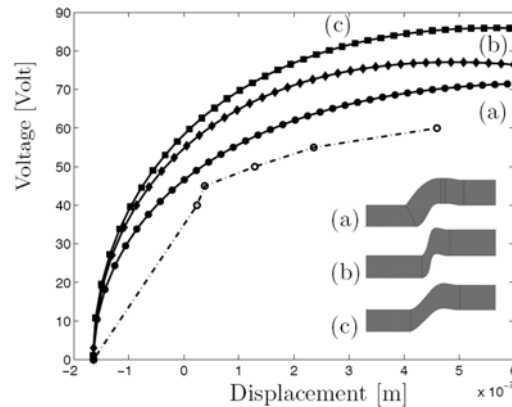


Figure 19: Pull-in curve for different shapes for the anchor of micro-bridge.

### 5.2 Poly1 Cantilever Micro-Beam

The second device treated here is a cantilever beam made in the layer Poly1. The initial configuration of the beam is relatively flat.

#### *Pull-in Curve*

The static electro-mechanical problem is solved using a Riks-Crisfield algorithm. The displacement of the extremity of the beam is plotted in Figure 20 when voltage increases. The numerical results are plotted in black dots, and the experimental results are in circles. The numerical results overestimate the experimental data.

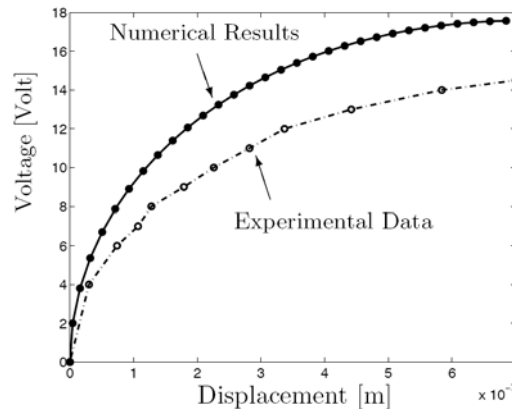


Figure 20: Pull-in curve for the cantilever beam.

### 5.3 Poly2 Cantilever Micro-Beam

We consider now a beam realized in the Polysilicon layer Poly2. The beam is thinner than the Poly1 ones, and the gap between the electrodes is larger.

#### *Pre-stress*

The beam is initially deformed due to a gradient of pre-stress inside the structure. In a cantilever beam, a uniform pre-stress as shown in Figure 21 is relaxed when the beam is released. To have an initial deformation of the beam such as in the measured initial configuration, a gradient of pre-stress such as in Figure 22 has to be added in the mechanical element.



Figure 21: Constant pre-stress.

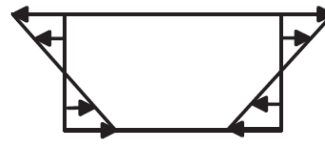


Figure 22: Gradient of pre-stress.

Using a Riks-Crisfield algorithm the beam is deformed as shown in figure 23. The deformation is magnified by 30. The maximum pre-stress necessary to achieve the measured deformation of the beam is about 2 MPa.



Figure 23: Initial deformation of the structure due to the pre-stress (30x).

#### *Pull-in Curve*

Starting from the pre-stressed beam the Riks-Crisfield algorithm is used to compute the deformation due to the electrostatic force. The displacement of the extremity of the beam is plotted in Figure 24 when the voltage increases. The black dots represent the numerical results and the circles the experimental data. The pre-stress bends the beam down so that the voltage needed to deform it is lower.

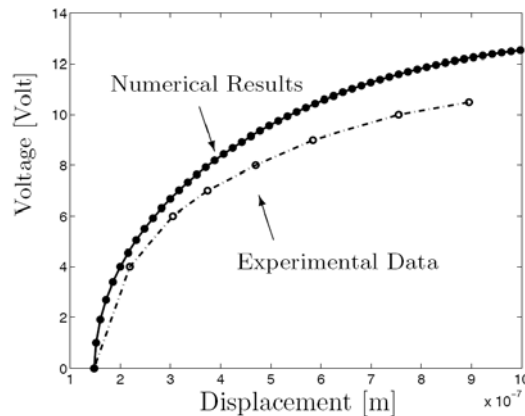


Figure 24: Displacement of the extremity of the beam due to the electrostatic forces.

#### **5.4 Model Updating**

In all the previous examples, the numerical results overestimate the experimental data. A lot of reasons may cause this difference namely the shape of the anchor, the dispersion on Young's modulus and other external parameters such as the ambient temperature. For a better agreement between numerical predictions and experimental results Young's modulus of the polysilicon is updated. The Poly1 cantilever beam is taken as reference beam, because no pre-stress influences its pull-in curve. To fit the experimental data of the Poly1 beam the Young's modulus is reduced to 112 GPa as shown in figure 25. The updated value of Young's modulus is then applied to the Poly2 cantilever beam problem. The gradient of pre-stress to obtain the measured displacement is reduced to 1.4 MPa on the surface. The numerical results fit very well the experimental data as shown in figure 25. By using the same Young's modulus for the micro-bridge the mean pre-stress is reduced to 22 MPa. The numerical results (line) and the experimental data (circle) are compared for the micro-bridge in Figure 25. The numerical results are in good agreement with experimental data.

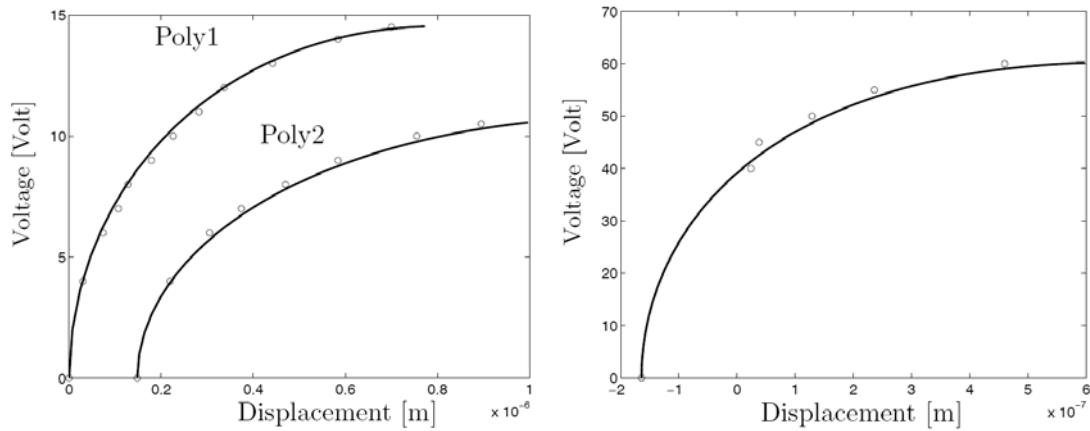


Figure 25: Comparison between the numerical (line) and experimental (circle) results for the cantilever beams and the micro-bridge.

## 6. Conclusion

This paper has shown the advantages of using a monolithically formulation to model electro-mechanical coupling effects in MEMS. Compared to classical staggered approaches, the proposed methodology allows a better understanding of the dynamic behavior of electrostatically-actuated MEMS devices and more specifically a better prediction of the dynamic and static pull-in voltages. It paves the way to a better design of such coupled systems using for example topology optimization tools.

## Acknowledgments

The first author acknowledges the financial support of the Belgian National Fund for Scientific Research. Part of the work presented in this text is also supported by the Communauté Française de Belgique – Direction Générale de la Recherche Scientifique in the framework Actions de Recherche Concertées (convention ARC 03/08-298).

## References

- [1] ANSYS, Training Manual Introduction to ANSYS 5.7 for MEMS, *First Edition ANSYS Release: 5.7, 2001*.
- [2] V. Rochus, D.J. Rixen, J.C. Golinval “Monolithical Modeling of Electro-Mechanical Coupling in Micro-Structures.” *International Journal for Numerical Methods in Engineering*.
- [3] W. S. Lee and K. C. Kwon and B. K. Kim and J. H. Cho and S. K. Young, “Frequency-shifting Analysis of Electrostatically Tunable Micro-mechanical Actuator,” *Journal of Modeling and Simulation of Micro-systems*, Vol. 2, No.1 (2001), pp. 83-88.
- [4] M. Geradin and D. J. Rixen, *Mechanical vibrations: Theory and Application to Structural Dynamics*, Wiley, *Second Edition*, 1997.
- [5] M. A. Crisfield, *Non-Linear Finite Element Analysis of Solids and Structures*, John Wiley 1991